Developing a passive load reduction blade for the DTU 10 MW reference turbine

J B de Vaal[1,2]**, T A Nygaard**[1] **and R Stenbro**[1]

[1] Institute for Energy Technology (IFE), Kjeller, Norway.
[2] Author to whom any correspondence should be addressed: jacobus@ife.no

Abstract. This paper presents the development of a passive load reduction blade for the DTU 10 MW reference wind turbine, using the aero-hydro-servo-elastic analysis tool 3DFloat. Passive load reduction is achieved by introducing sweep to the path of the blade elastic axis, so that out-of-plane bending deflections result in load alleviating torsional deformations of the blade. Swept blades are designed to yield similar annual energy production as a rotor with a reference straight blade. This is achieved by modifying the aerodynamic twist distribution for swept blades based on non-linear blade deflection under steady state loads. The passive load reduction capability of a blade design is evaluated by running a selection of fatigue- and extreme load cases with the analysis tool 3DFloat and determining equivalent fatigue loads, fatigue damage and extreme loads at the blade root and tower base. The influence of sweep on the flutter speed of a blade design is also investigated. A large number of blade designs are evaluated by varying the parameters defining the sweep path of a blade's elastic axis. Results show that a moderate amount of sweep can effectively reduce equivalent fatigue damage and extreme loads, without significantly reducing the flutter speed, or compromising annual energy production.

1. Introduction

In order to minimise the cost of wind energy conversion, it is of interest to design rotor blades that maximise energy extraction from the wind while minimising operational loads. To this end, passive load reduction by means of coupling between blade bending and twisting, are of primary interest.

The intent of a blade with bend-twist coupling is to (passively) reduce aerodynamic loads resulting from sudden inflow changes that can be attributed to e.g. turbulent inflow or wind gusts. By coupling the bending and torsional responses of a blade such that out-of-plane bending due to aerodynamic loading causes torsional deflection that reduces aerodynamic loads (by changing the aerodynamic angle of attack), passive load reduction is obtained. Typically, this desired bend-twist coupling is obtained either through the use of anisotropic structural/material properties [1] or by creating an offset between the local aerodynamic pitch- and blade pitch axes [2]. The latter approach of applying backward sweep to the blade is the approach followed in the current work.

The effectiveness of this technique has been illustrated in actual designs [3] [4] as well as in various numerical studies on reference blades [5] [6] [7] [8]. These previous studies have also indicated some of the potentially undesirable consequences of bend-twist coupling. Due to the coupling between bending and twisting, an otherwise optimal blade twist distribution is modified and can potentially result in a reduction of the annual energy production [1]. This should be taken into account when comparing the load reduction effectiveness of different blade designs [6]. Another undesirable dynamic effect of bend-twist coupling is a reduction in the rotor speed where classical flutter [7] and other aeroelastic instabilities [8] occur.

2. Method

In this work, a parameter study approach for developing a passive load reduction blade is presented, illustrated by application to the DTU 10 MW reference turbine [9], using a state of the art finite element based aero-hydro-servo-elastic analysis tool, 3DFloat.

2.1. Description of the simulation tool 3DFloat

The structural model in 3DFloat is a nonlinear corotational FEM framework, where computational nodes are interconnected with Euler-Bernoulli beam elements with 12 Degrees-of-Freedom (DOF). Time domain computations are carried out using the implicit Generalized-α method, with modified Newton sub-iterations for solution convergence within each time-step, governed by a residual criterion [10]. The beam model takes into account offsets in mass-, shear-, and aerodynamic centres from the elastic axis, to ensure realistic modelling of e.g. wind turbine blades [11]. Loads from e.g. gravity and wind are applied as distributed external loads on the structure. Forces are evaluated at Gauss points in the elements, and a Galerkin approach is used to evaluate consistent nodal loads. Wind is handled as a nonlinear drag term on structural elements representing the wind turbine, apart from the blades which are modelled with airfoil elements using aerodynamic lift-, drag- and moment coefficient lookup tables. Currently, 3DFloat does not include any unsteady profile aerodynamics (or dynamic stall) models. The induced velocity for wind turbine rotors is computed with Blade Element/Momentum (BEM) theory, with enhancements for dynamic inflow and yaw errors [12] [13]. Turbulence in the wind is modelled by importing turbulence files generated with MannSim.

2.2. Defining blade sweep

The sweep of the blade aerodynamic pitch axis is defined according to the power law equation (1) as in [7] using three parameters to define the sweep shape: linear forward sweep, a, total backward sweep, b and distribution of sweep along the blade, c:

$$y(z, a, b, c) = a\left(\frac{z-z_0}{z_{tip}-z_0}\right) - b\left(\frac{z-z_0}{z_{tip}-z_0}\right)^c \quad (1)$$

Parameters b and c define the backward sweep that gives beneficial structural coupling between blade flapwise- and torsional bending, while parameter a gives linear forward sweep to counter steady state twisting moments on the blade resulting from the backward sweep.

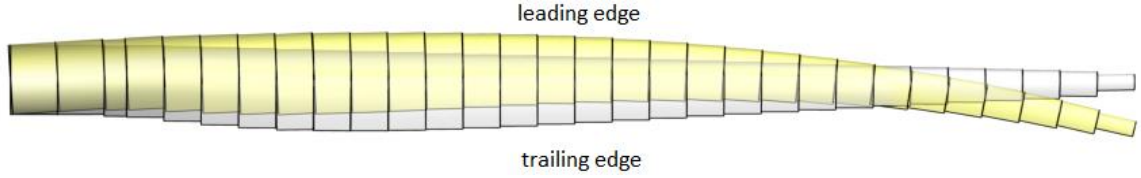

Figure 1. View of the suction sides of the baseline and a swept blade ($\boldsymbol{a = 0.06}$, $\boldsymbol{b = 0.10}$ and $\boldsymbol{c = 3.0}$) illustrating forward sweep inboard and backward sweep outboard towards the blade tip.

2.3. Parameter study approach

A parameter study is performed to determine the influence of the forward- and backward sweep parameters on various performance measures of a rotor. The backward sweep distribution parameter $c = 3$ is chosen so that blade sweep angle (proportional to the sweep curvature) increases linearly towards the tip of the blade.

Table 1. Parameters used to define the blade sweep, normalised with normal distance from hub centre, $z_{tip} = 89.166\,m$, where applicable.

Parameter	Normalised values [-]	Values [m]
forward sweep – a	0.02, 0.04, 0.06, 0.08	1.783, 3.567, 5.350, 7.133
backward sweep – b	0.08, 0.10, 0.12, 0.14	7.133, 8.917, 10.700, 12.483
Sweep distribution – c	N/A	3.0

For each sweep design, based on a unique combination of parameters from Table 1, the aerodynamic twist distribution is modified, to ensure that energy production is not compromised. Then, the same normal- and extreme wind conditions are simulated and the resulting fatigue- and extreme- loads are determined. During these simulations, rotor speed and blade pitch are controlled using the DTU Wind Energy controller [14] with identical parameter settings for all blade designs. To further assess the influence of blade sweep on the aeroelastic behaviour of the rotor, a runaway test (loss of generator torque and blade pitch control) is simulated to find a rotor speed where aerodynamic instabilities occur for each blade design. Finally, all blade designs resulting from the parameter study are compared relative to the baseline/reference blade, allowing trends to be established between sweep geometry and the resulting influence on loads, performance and aerodynamic stability.

2.4. Modification of aerodynamic twist

Backward sweep is intended to reduce loads on blades, however, this can also lead to a reduction in the power produced by the wind turbine. For a fair comparison, it is important to ensure that loads from turbines that produce equal power are compared to each other.

In the current work, (near) equal power production is achieved by modifying the aerodynamic twist distribution for each sweep design. Once a blade sweep path is defined, a steady state simulation in a uniform wind at the average wind speed of the selected wind class (IEC IA, $V_{ave} = 10\,m/s$) [15] is performed and the twist deformation along the blade span is determined. The difference between the twist deformation of the reference blade and a swept blade is added to the blade aerodynamic twist for all following simulations with a swept blade, effectively ensuring that energy production is not compromised. An example of this is shown in Figure 2 where the swept blade considered is identified by the parameters, see equation (1), defining its shape.

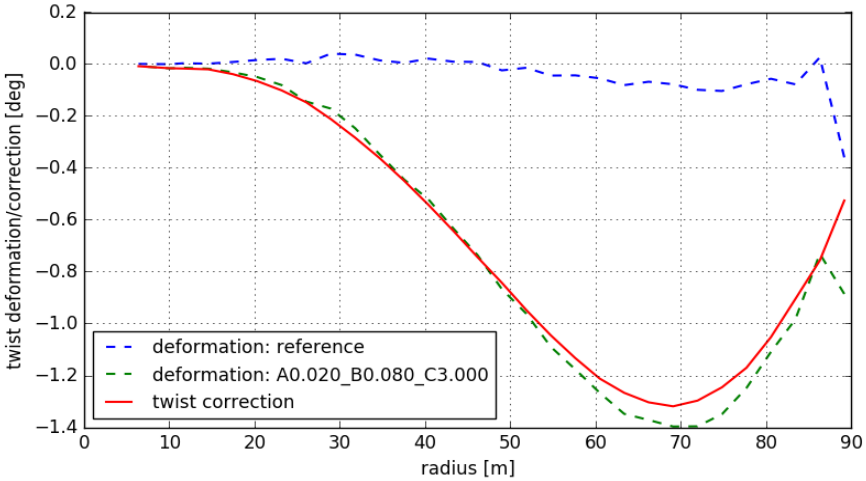

Figure 2. Steady state elastic twist deformation (at $\boldsymbol{V_{hub} = 10\,m/s}$) along the blade span for the reference blade and a swept blade (defined by a=0.02, b=0.08 and c=3), indicated by dashed lines. The correction to the aerodynamic twist (difference between the reference- and swept blade deformation) that is subsequently applied for the swept blade is indicated by the solid line.

2.5. Load cases and environmental conditions considered

The load cases considered in the current work are summarized in Table 2. These load cases are selected to give a basis from which performance with respect to fatigue- and ultimate/extreme loads can be compared for different blade designs. For the operational load cases, ten different wind speeds (see Figure 3) covering the operational wind speed range of the DTU 10 MW turbine are considered. In case turbulence is modelled, two unique random seeds are used per wind speed. For the deterministic wind load cases, wind gust magnitude and directions are determined as defined in [15]. A slowly increasing deterministic wind is used for the rotor runaway simulation.

Table 2. A brief description of the load cases considered for analysis, including wind speeds, direction and analysis type.

#	Load case description	Wind speed(s) [m/s]	Wind direction	Type of analysis
1	Normal turbulence model	$6, 8, 10, 12, 14, 16, 18, 20, 22, 24$	Turbulent	Fatigue
2	Extreme turbulence model	$6, 8, 10, 12, 14, 16, 18, 20, 22, 24$	Turbulent	Ultimate
3	Extreme coherent gust with direction change	$8, 10, 12, 14, 16, 18$	+,-	Ultimate
4	Extreme operating gust	$8, 10, 12, 14, 16, 18$	N/A	Ultimate
5	Rotor runaway	$4.5 - 15.0$ (during $2250\ sec$)	0	Flutter

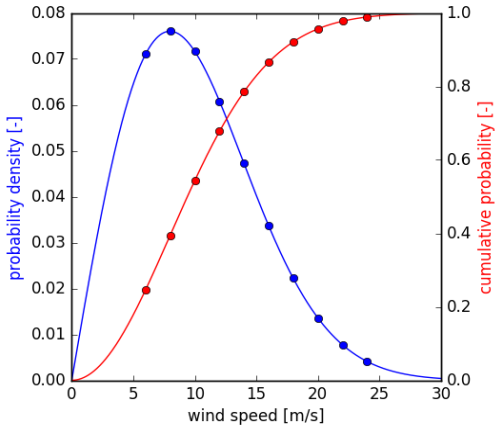

Figure 3. Rayleigh probability distributions for wind speed for IEC class I with $\boldsymbol{V_{ave} = 10\ m/s}$. Circular markers indicate wind speeds simulated.

3. Results

Results will be compared at three locations: the tower base, the tower top and the blade root. In this results section, all comparisons for different swept blade designs are made relative to results for the baseline rotor. Results are presented as percentage difference from the reference case, according to equation (2):

$$\%difference = \left(\frac{x}{x_{ref}} - 1\right) \times 100 \tag{2}$$

3.1. Performance of the baseline rotor

Summarized properties for the baseline rotor are presented in Table 3.

Table 3. Summarized results for the baseline rotor, consisting of design equivalent loads and extreme loads at the tower base, tower top and blade root.

Location	Load component	Fatigue 20-year DEL [kNm]	Extreme load [kNm]
Tower base	Torsional moment	833.76	-47724.61
	Fore-aft moment	1178.97	307792.09
	Side-to-side moment	960.46	-105186.90
Tower top	Torsional moment	830.31	-47433.07
	Fore-aft moment	831.82	45022.80
	Side-to-side moment	420.59	-15212.88
Blade root	Torsional moment	56.34	831.76
	Flapwise moment	3186.34	-51415.01
	Edgewise moment	2276.69	20321.41
Rotor speed at instability		23.80 rpm	

3.2. Fatigue loads

Loads from simulations with wind according to the Normal Turbulence Model are used for fatigue damage calculations. To compare the relative performance of different blade designs with the reference blade, without taking the detailed design of structural components into account, 20-year design equivalent loads (DEL) are calculated. Based on the Palmgren-Miner damage summation rule, a design equivalent load is a load that at a chosen equivalent number of cycles, here $N_{eq} = 10^7$, will give the same damage as the summation of the k cycles $N_{i,k}$ of load ranges $S_{i,k}^m$ determined using rainflow counting [16]. In equation (3), subscript i refers to simulations at a wind speed in Table 4, simulated for a total duration of $T_{sim,i}$, representing $T_{life,i}$ of operation during a scaled 20-year lifetime [9].

$$DEL = \left(\frac{1}{N_{eq}} \sum_{i=1}^{N_{v_i}} \left(\frac{T_{life,i}}{T_{sim,i}} \sum_{k=1}^{N_k} N_{i,k} S_{i,k}^m\right)\right)^{\frac{1}{m}} \quad (3)$$

Table 4. Scaled wind speed distribution during 20-year lifetime, and time simulated.

Wind speed [m/s]	Minutes during 20-year lifetime
5 - 7	1686097
7 - 9	1814258
9 - 11	1705167
11 - 13	1452501
13 - 15	1128334
15 - 17	804490
17 - 19	537139
19 - 21	327082
21 - 23	186650
23 - 25	99783

The material specific Wöhler coefficient m in equation (3), is set to $m = 3$ for calculations on the tower, and to $m = 10$ for the blade root – the same as in [9]. A relative change in DEL can also be expressed, as a change in relative lifetime:

$$\frac{T}{T_{ref}} = \left(\frac{DEL}{DEL_{ref}}\right)^m \quad (4)$$

From equation (4) it is easy to grasp that, especially if exponent *m* is large, a small reduction in DEL leads to a large reduction of the used fatigue life.

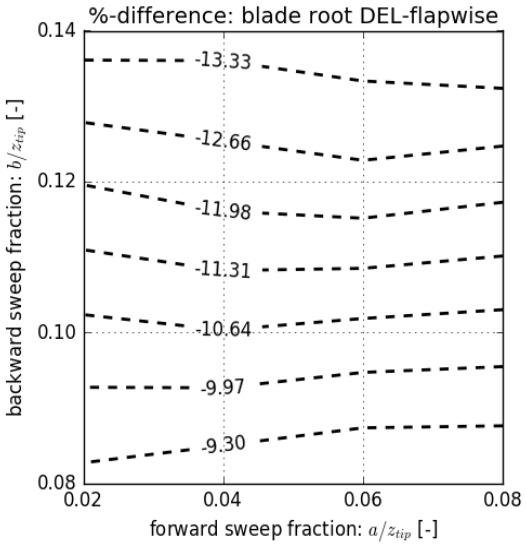

Figure 4. Change from baseline flapwise design equivalent fatigue moment at the blade root

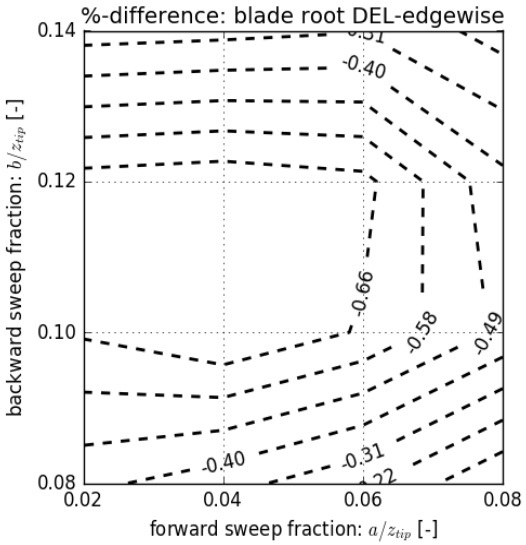

Figure 5. Change from baseline edgewise design equivalent fatigue moment at the blade root

The contours in Figure 4 show that the blade root flapwise design equivalent loads are reduced by approximately 9%-13% with respect to the baseline rotor, depending on the values of the sweep factors *a* and *b*. Increasing the backward sweep has the largest effect in reducing the fatigue load. There is only a marginal change in the edgewise design equivalent fatigue load, as shown in Figure 5.

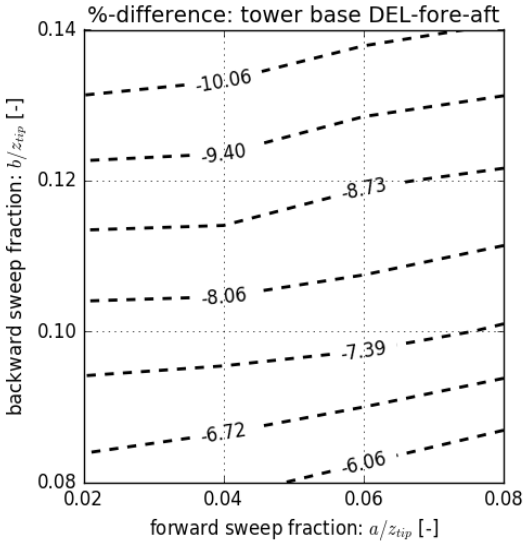

Figure 6. Change from baseline fore-aft design equivalent fatigue moment at the tower base.

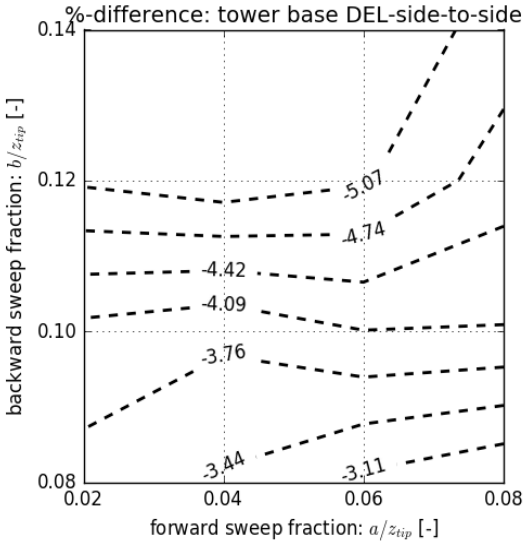

Figure 7. Change from baseline side-to-side design equivalent fatigue moment at the tower base.

At the tower base, there are also reductions in design equivalent fatigue loads, for the range of sweep parameters considered. The reduction in loads at the blade roots, translates into reductions of the fore-aft, Figure 6, and side-to-side, Figure 7, tower base equivalent fatigue moments. Larger reductions are

obtained by increasing the blade backward sweep, while increasing the linear forward sweep marginally reduces the gains achieved by backward sweep.

Changes from baseline torsional design equivalent moments at the blade root and tower base are shown in Figure 8 and Figure 9, respectively. Note although there is a dramatic increase in torsional fatigue load at the blade root, due to adding backward sweep, it is an increase from a very small baseline number. At the tower base, reductions in torsional load are of similar magnitude as the reductions of moments along the fore-aft and side-to-side axes.

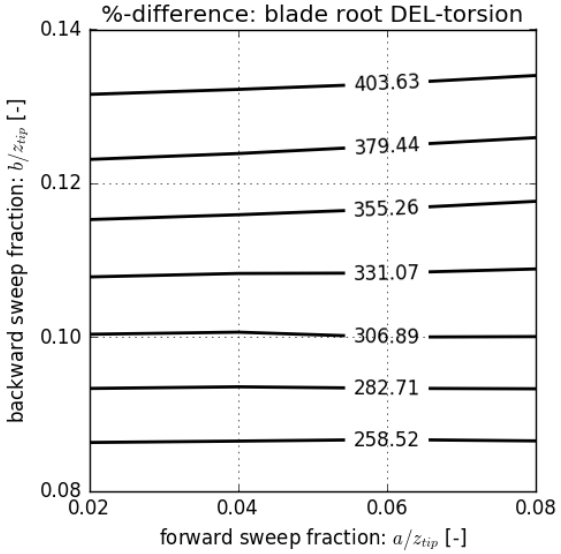

Figure 8. Change from baseline torsional design equivalent fatigue moment at the blade root

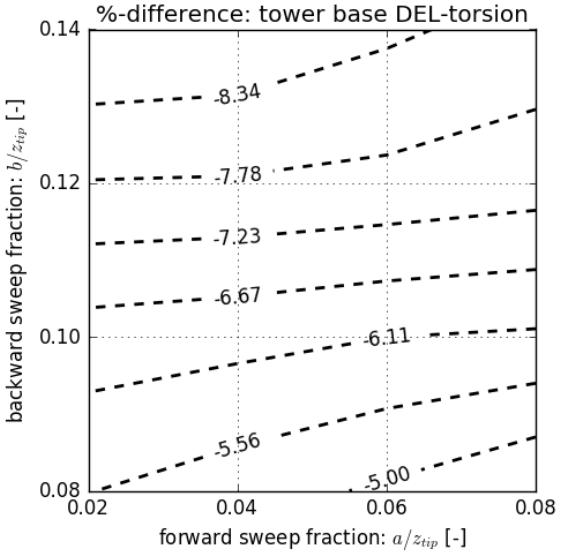

Figure 9. Change from baseline torsional design equivalent fatigue moment at the tower base

3.3. Extreme loads

Extreme loads for moments about all three structural axes at each of the monitoring locations considered, were determined by recording the load with the largest absolute value occurring during any of the first four load cases considered (see Table 2). For blade loads, the largest value measured on any of the three blades is reported. Comparisons made to extreme loads in the baseline case do therefore not necessarily refer to the loads from the same blade, load case, or environmental condition, only the overall load magnitude.

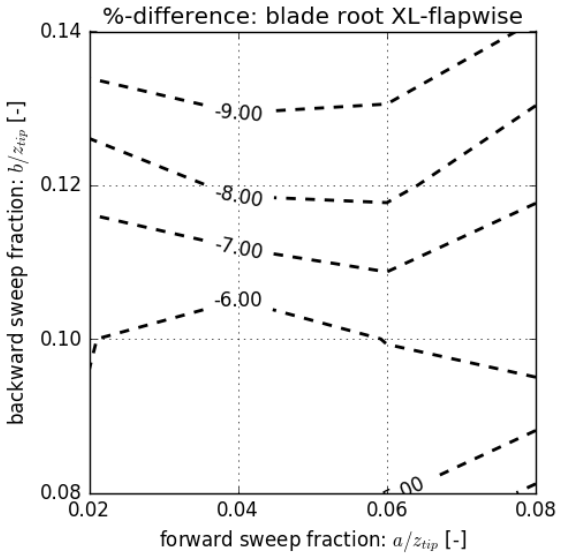

Figure 10. Change from baseline extreme flapwise moment at the blade root

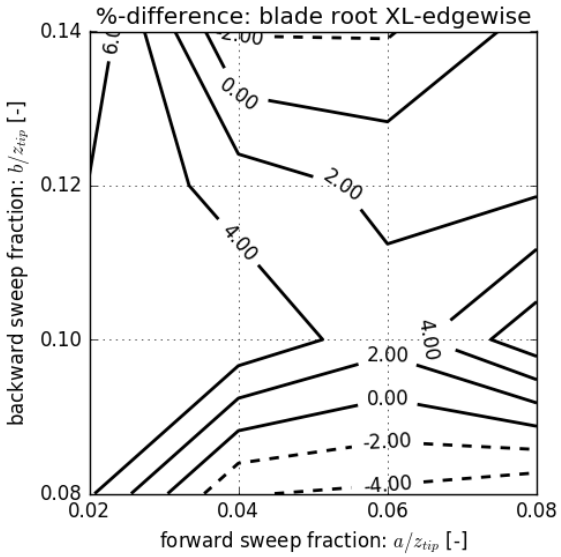

Figure 11. Change from baseline extreme edgewise moment at the blade root

The contours in Figure 10 show that extreme flapwise moments are reduced between approximately 5% and 9%, whereas Figure 11 shows an increase of up to 4% for extreme edgewise moments at the blade root, when comparing to the baseline case. It is important to note that the extreme edgewise moments have a much smaller magnitude than the extreme flapwise moments.

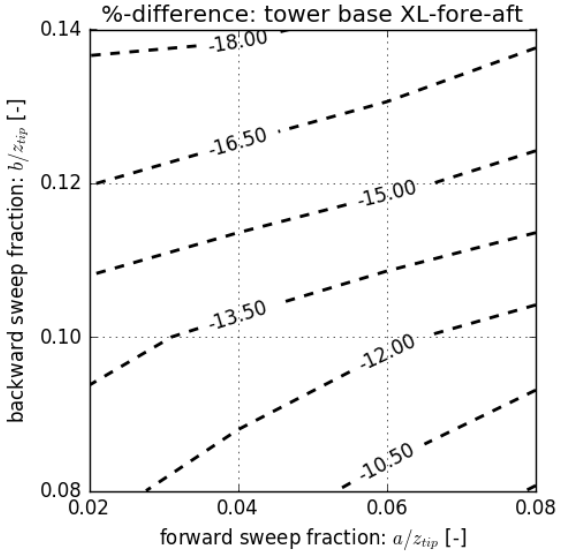

Figure 12. Change from baseline extreme fore-aft moment at the tower base

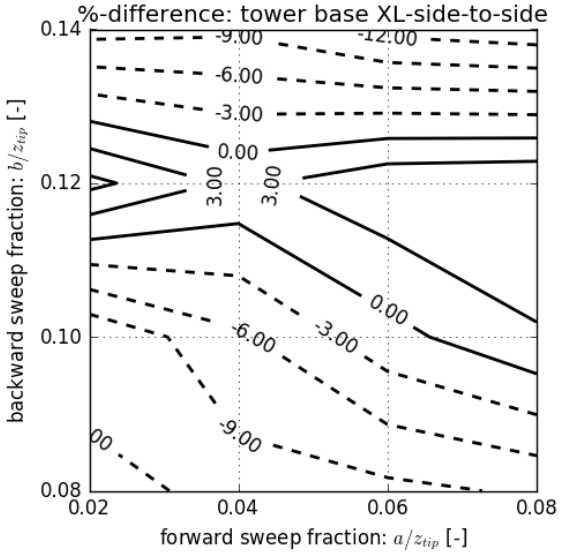

Figure 13. Change from baseline extreme side-to-side moment at the tower base

At the tower base, Figure 12 shows that the extreme fore-aft moments are reduced by between 10% and 18%, compared to the reference blade. For the tower base side-to-side moment, reductions as well as increases in extreme moments are observed, depending on the value of the sweep coefficients. In magnitude, the side-to-side moment is smaller than the fore-aft moment, and as such a slight increase in side-to-side moment is not significant.

3.4. Aerodynamic instability

A simple test for rotor aerodynamic instabilities was set up by simulating a rotor runaway case, where generator torque is removed and blade pitch control deactivated. The wind speed is slowly increased, allowing the rotor to spin up freely and increase its rotational speed as the wind speed increases. This continues until aerodynamic loads are of such a nature structural damping alone is not sufficient to suppress any aeroelastic instabilities. For all the blade designs the rotor speed at which instabilities start to occur was determined, and compared to that of the baseline rotor. The results are shown in Figure 14, and indicate that the rotor speed for aerodynamic instabilities is marginally reduced by introducing blade sweep. Since this rotor speed for the baseline blade is more than double the rated rotor speed, the observed difference for swept blades are not considered to be of primary importance.

For the reference blade, there are known edgewise aerodynamic instabilities when the rotor is in a parked state during storm winds [9]. In the reference description, it is suggested that active control could be used to suppress these instabilities [9]. For that same reason, because of inherent uncertainty in accurate modelling of parked rotor blades using a blade element based approach, and due to the lack of a dynamic stall model in the simulation tool 3DFloat, it was decided to not investigate the parked blade instabilities for the swept rotor blade designs in the current work, even though it could be a load case of significance.

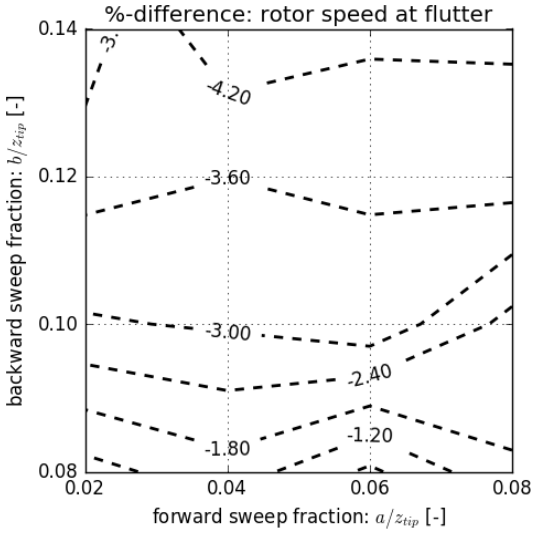

Figure 14. Change from baseline rotor speed at which aerodynamic instability occurs

3.5. Power production

In Figure 15, the average electrical power produced during normal turbulence model load cases, weighted according to the probability of occurrence for each wind speed considered, as compared to the baseline case is presented.

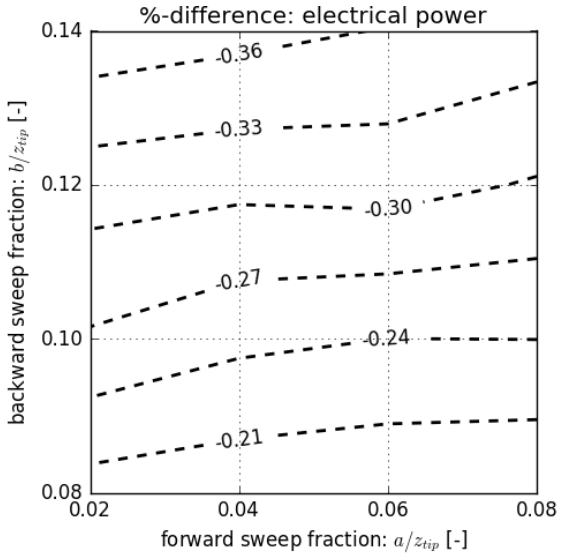

Figure 15. Change from baseline electrical power produced during the power production load cases

It shows that the design objective of maintaining near constant power production, regardless of blade sweep, was largely achieved. This implies that comparisons of loads were done for rotors with equivalent performance, and that load reductions are due to improved blade aeroelastic behaviour and not mainly due to reduced performance.

4. Conclusions

This paper described an approach for designing a passive load reduction blade for the DTU 10 MW reference turbine, by applying backward sweep to the rotor blades. It was assumed that structural and aerodynamic properties for swept blades are the same as for the baseline rotor blade. However, the aerodynamic twist of swept blades was modified to ensure that power production was not compromised significantly. A parameter study was then performed to compare different blade sweep designs to the baseline blade. This was done by comparing loads at key locations on the turbine, for a predetermined number of load cases, covering fatigue and extreme loads. The main conclusions that were reached are:

- Reductions in flapwise design equivalent loads at the blade root in the order of 10% are achievable. This translates to a potentially significant increase in the fatigue life. There is, however, a large increase in the torsional loads on the blade root.
- Flapwise extreme moments at the blade root can also be reduced by up to 10%, while edgewise moments are increased by up to 4% - although these are smaller in magnitude. The extreme torsional moments, that are very small for the baseline blade, are increased by up to 240%. While these increases may not be significant for the blade construction itself, it could be of more importance for the blade pitch mechanism.
- At the tower base, reductions in design equivalent fatigue loads were observed for moments about all axes in the range of 3% to 10%. Extreme loads were reduced by a larger margin, although small increases were also observed in the side-to-side moment.
- Based on rotor runaway simulations, aerodynamic instabilities were found to occur at rotor speeds up to approximately 5% lower than for the baseline rotor blade. However, since this is still at a rotor speed that is more than double the rated speed, the introduction of blade sweep does not appear to be critical. Other aerodynamic instabilities were not investigated.

The presented results give a promising outlook for incorporating a certain amount of backward sweep into rotor blades. However, more detailed investigations should be done to ensure the structural

feasibility of applying blade sweep to the DTU 10 MW reference turbine. For example, distribution of blade loads along the length of the blade was not considered in the current investigation. And local phenomena, such as buckling, were not investigated. The results generated during this study do, however, indicate possibilities and can be used as input for more detailed future studies.

References

[1] Lobitz DW and Veers PS, 1998, Aeroelastic behavior of twist-coupled HAWT blades, 1988 ASME Wind Energy Symposium, no. 98-0029.

[2] Zutek M, 2002, Adaptive blade concept assessment: curved platform induced twist investigation, Sandia National Laboratories, SAND2002-2996.

[3] Ashwill TD, 2010, Sweep-twist adaptive rotor blade: final project report, Sandia National Laboratories, SAND2009-8037.

[4] Siemens AG, 2012, Siemens aeroelastically tailored blade: Innovative blade increases, online: http://www.energy.siemens.com/mx/pool/hq/power-generation/renewables/wind-power/aerolastically_tailored_blades_brochure.pdf.

[5] Verelst DR and Larsen TJ, 2010, Load consequences when sweeping blades-A case study of a 5 MW pitch controlled wind turbine, Risø DTU, Risø-R-1724(EN).

[6] Pavese C and Kim T, 2014, Implementation of passive control strategies through swept blades, in 10th EAWE PhD Seminar on Wind Energy in Europe.

[7] Hansen M, 2011, Aeroelastic properties of backward swept blades, in Proceedings of 49th AIAA Aerospace Sciences Meeting Including The New Horizons Forum and Aerospace Exposition.

[8] Larwood S, Van Dam C and Schow D, 2014, Design studies of swept wind turbine blades, *Renewable Energy*, **71**, 563-571.

[9] Bak C, Zahle F, Bitsche R, Kim T, Yde A, Henriksen LC, Natarajan A and Hansen MH, 2013, Description of the DTU 10 MW Reference Wind Turbine, DTU Wind Energy, Report-I-0092.

[10] Nygaard TA, De Vaal JB, Pierella F, Oggiano L and Stenbro R, 2016, Development, Verification and Validation of 3DFloat; Aero-Servo-Hydro-Elastic Computations of Offshore Structures, in 13th Deep Sea Offshore Wind R&D Conference, EERA DeepWind, Trondheim, Norway.

[11] Söderberg M, 1989, Implementation of Shear Offset and Rigid Offset for Beam Element in Finite Element Code GARFEM, FFA TN 1989-24, The Aeronautical Research Institute of Sweden.

[12] Hansen MOL, Sørensen JN, Voutsinas S, Sørensen N and Madsen HA, 2006, State of the art in wind turbine aerodynamics and aeroelasticity, *Progress in Aerospace Sciences*, **42(4)**, 285-330.

[13] Björck A, 2000, AERFORCE: Subroutine Package for unsteady Blade-Element/Momentum Calculations, The Aeronautical Research Institute of Sweden, FFA TN 2000-07.

[14] Hansen MH and Henriksen LC, 2013, Basic DTU Wind Energy controller, DTU Wind Energy E-0028.

[15] Anonymous, 2005, Wind turbines - Part 1: Design requirements, IEC 61400-1:2005(E), International Electrotechnical Commission.

[16] Brodtkorb PA, Johannesson P, Lindgren G, Rychlik I, Rydén J, Sjö E and others, 2000, WAFO-a Matlab toolbox for analysis of random waves and loads, in The 10th ISOPE Conference.